Available online at sjuoz.uoz.edu.krd

journals.uoz.edu.krd

Science Journal of University of Zakho

Vol. 11, No. 1, pp. 73– 77, January-March 2023

p-ISSN: 2663-628X
e-ISSN: 2663-6298

NANOSTRUCTURED SILVER THIN FILM: USING SUCCESSIVE IONIC LAYER ADSORPTION AND REDUCTION METHOD

Ari A. Yatem [a,*] and Mohammed Noor S. Rammoo [a]

[a] Department of Physics, Faculty of Science, University of Zakho, Zakho, Kurdistan Region, Iraq
(ari.yatem@uoz.edu.krd)

Received: *29 Sep., 2022 /* ***Accepted:*** *20 Oct., 2022 /* ***Published:*** *30 Jan., 2023* ***https://doi.org/10.25271/sjuoz.2022.11.1.1017***

ABSTRACT

The Successive Ionic Layer Adsorption and Reduction (SILAR) method was utilized to produce nanostructured silver thin films on a glass substrate. Ag nanoparticles were grown using SILAR parameters such as silver nitrate ($AgNO_3$), reduction time, reduction agent in an aqueous solution of hydrazine hydrate with various concentrations, and growth cycles. In this study, X-ray diffraction (XRD), scanning electron microscopy (SEM), and UV-visible-NIR absorption spectroscopy techniques were used to assess the produced silver thin film nanostructure. The size and spreading of the formed silver nanoparticles are observed to grow with the reducing agent and eventually saturate for constant growth cycles. As a result, the size and the distribution of the produced Ag nanoparticles grow uniformly. Higher growth cycles, however, caused Ag nanoparticles to lose their homogeneity and change into gravel-shaped particles. Therefore, silver nanoparticles that have been produced with the ideal SILAR conditions can be employed as an extremely sensitive, repeatable substrate with an exceptionally efficient factor. Moreover, the Effect of the concentration of HyH on the properties of SILAR-grown silver thin films has been extensively studied.

KEYWORDS: SILAR, Silver nanoparticles, Reducing agent, Surface Plasmon Resonance, Growth cycle.

1. INTRODUCTION

Nanoparticles have inspired a great deal of interest in both science and commerce because they exhibit incredibly intriguing and practical qualities that bulk materials cannot, which may be used for a wide range of purposes [1]. Those with physical characteristics in a micrometer range mostly resemble materials in bulk; however, those with physical characteristics in the nanometer range are various in the bulk form [2]. At the range of nano, the proportion of surface atoms or ions increases noticeably to the total atoms or ions and the characteristics of such materials are strongly influenced by surface energy. Due to the change in the characteristics, the ratio rises in the surface to the volume. Contrary to significant energy levels in bulk materials, the electrical structure of materials is also altered at the range of nano, leading to the emergence of discrete energy levels [3]. Nanoparticles (NPs) display numerous fundamental properties such as optical, electrical, magnetic, and thermal conductivity, etc. These intriguing characteristics of nanomaterials are highly influenced by their shape, the size of nanoparticles, interactions with stabilizers, and the environment, as well as how they were made [4]. Many recent types of research on the synthesis of nanoparticles (NPs) and studying their properties and size have shown that some of the properties of nanoparticles such as magnetic, catalytic, electronic, and optical depend on their shape, size, chemical environments, as well as the morphology of NPs [5]. Due to their potential uses in optical, medical, and electrical devices, metal nanoparticles (MNPs) (such as Ag, Au, or Cu NPs) have gained a lot of attention in a variety of fields. A significant number of publications have been published on the creation of metal nanoparticles of varied morphologies, and controlling their size and shape is a difficult task [6]. Among the mentioned metal NPs silver (Ag) nanoparticles have drawn the most attention because of their numerous applications in multi-disciplines including industrial, and their fascinating physical and chemical characteristics [7]. Silver nanostructures are typically grown from the solution of silver ions. The Ag^+ is produced from salt, for instance, silver nitrate ($AgNO_3$). At first, the ions are converted to atoms in this case a reducing agent will be utilized. The acquired atoms then start to form tiny clusters, which develop later into particles. The size and shape of the nanoparticles may be modified based on the number of atoms, which in turn depends on the silver salt to reduce the agent concentration ratio. In this process, a reducing agent and a silver salt are required for the nanoparticle to be grown [8]. Many techniques have already been studied for the preparation of silver nanoparticles such as metal vapor deposition, photochemical, sputtering, sol-gel, chemical reduction, ion implantation, microwave-assisted synthesis, laser ablation, and thermal decomposition [9]. Each technique has advantages and disadvantages, but they all have issues with cost, stability, uniform particle size, and size dispersion [10]. The chemical methods have been the most widely employed for the manufacture of Ag-NPs. The most accessible and all-encompassing method for creating metal nanoparticles is the chemical reduction of metal ions [11]. Silver ions can be chemically transformed into silver nanostructures by utilizing the Successive Ionic Layer Adsorption and Reduction (SILAR) method [12]. Our primary goal in this study is to establish the sustainability of the successive ionic layer adsorption and reduction (SILAR) method for growing Ag nanoparticles with the help of SILAR parameters in the growth cycles such as silver nitrate ($AgNO_3$), reduction time, reduction agent in an aqueous solution with various concentrations of hydrazine hydrate. In addition, it aims to study the effect of hydrazine hydrate concentrations on the properties of SILAR-grown Ag thin film. The most straightforward solution technique for

---

* Corresponding author

growing metal nanoparticle films on wide-area substrates is SILAR [13]. When using the SILAR method to produce MNPs, the reduction of metal ions pre-adsorbed on the surface only occurs on the surface of the substrate to prevent material loss in the form of precipitation. This is crucial for the growth of precious metal nanoparticles with the less expensive technique. The formation of metal/semiconductor thin films is controlled by several factors, including the precursor concentration, immersion duration, growth cycles, and temperature [14]. According to reports, the SILAR technique has been utilized to grow Ag nanoparticles for a variety of uses [15].

2. EXPERIMENTAL DETAILS

Ag thin film nanostructure was applied to the glass substrate. It has utilized silver nitrate ($AgNO_3$) as a silver ion source, and an aqueous solution of hydrazine hydrate (HyH) with various concentrations (0.01 M, 0.1 M, and 1.0 M) at a constant concentration (0.01 M) of aqueous $AgNO_3$. Several reducing agents can be utilized to reduce silver ions such as hydrazine hydrate [16], sodium borohydride [17], amino acid [18], ethylene glycol [19], and glucose [20] to get Ag nanoparticles. All the chemical materials used in this research were purchased from the Sigma Aldrich company and directly utilized with no further purification [purity 99%]. The glass slides were purchased from the Blue Star company with a dimension of (2.5 x 7.5) cm. Before the deposition process, the glass slides were cleaned and sonicated in distilled water. A growth cycle of Ag thin film nanostructure can be divided into four stages, as shown in figure 1.

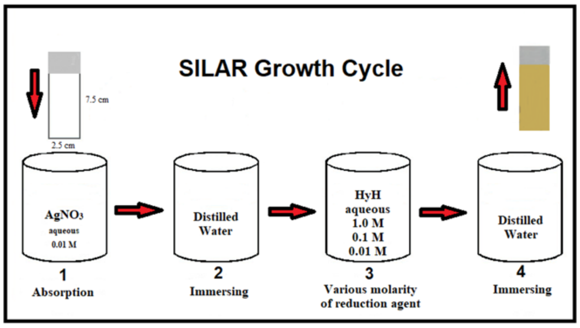

Figure 1. Schematic of the method for growing Ag nanoparticles using successive ionic layer adsorption and reduction. The growth cycle can be divided into four stages: (1) Absorption, (2) Immersing, (3) Reduction agent with various concentrations, and (4) Immersing.

The glass slide substrate was initially submerged in an aqueous solution of $AgNO_3$ for about 15 sec, which caused Ag+ ions to adsorb the substrate. To remove weakly adsorbed ions, the glass substrate was next submerged in a beaker of distilled water for about 30 sec. After the rinse stage, the substrate is submerged in the aqueous hydrazine hydrate solution for about 15 sec, to decrease the highly adsorbed ions on the substrate. Lastly, to eliminate loosely linked Ag nanoparticles or any other weakly adsorbed ionic compounds, the substrate was once more cleaned with distilled water and retained in a separate beaker for about 30 sec. This ends a cycle of SILAR growth. The growth cycle was repeated three times for different concentrations (0.01 M, 0.1 M, and 1.0 M) of aqueous hydrazine hydrate solution at a constant concentration (0.01 M) of aqueous $AgNO_3$. The impacts of reducing time and growing cycle for the optimum precursor concentrations have been investigated since these factors greatly affect the size and distribution of the produced Ag nanoparticles, as shown in Table 1.

Table 1. Optimization parameters of SILAR method for growing Ag nanoparticles.

SILAR growth cycle parameters	**Values**
The concentration of aqueous $AgNO_3$	0.01 M
The concentration of aqueous hydrazine hydrate	0.01 M 0.1 M 1.0 M
Adsorption Time	15 sec
Immersing Time	30 sec
Reduction Time	15 sec
Growth Cycle	3

In the present work, the thickness of the film was measured at 141±8 nm by the gravimetric weight difference method using the relation [21]:

$$t = m / \rho * A \qquad (1)$$

where (m) is the mass of the film deposited on the substrate in gm. (A) is the area of the deposited film in cm^2 and ρ is the density of the silver.

The following are the chemical reactions used in the SILAR method to grow Ag nanoparticles. $AgNO_3$ is decomposed and produces Ag+ ions when it dissolves in water [22], which can be expressed as:

$$AgNO_3 \longrightarrow Ag^+ (aq.) + NO_3^- (aq.) \quad (2)$$

Hydrazinium ions are generated in hydrazine hydrate aqueous solution and produce electrons that are then utilized to reduce Ag+ ions as shown in the following reactions:

$$N_2H_4 + H_2O \longrightarrow N_2H_5^+ + OH^- \qquad (3)$$

$$N_2H_5^+ \longrightarrow N_2 + 5H^+ + 4e^- \qquad (4)$$

Thus, the following overall response may be used to express the Ag nanoparticle growth [23]:

$$4AgNO_3 + N_2H_4 \longrightarrow 4Ag + 4HNO_3 + N_2\uparrow (5)$$

The silver thin film nanostructures were characterized by the X-ray diffraction (XRD) technique. Scanning Electron Microscope (SEM) images were done to investigate the surface morphology of the produced Ag nanoparticles. The UV-Vis-NIR spectrophotometer was used to detect the optical absorption of the generated Ag nanoparticles.

3. RESULTS AND DISCUSSIONS

3.1. Characterization of thin film by X-Ray diffraction (XRD)

X-Ray Diffraction (XRD) has been utilized to characterize the produced Ag thin films nanostructure with the help of a Bruker D8 advanced diffractometer. Figure 2 shows (XRD) pattern of Ag thin film nanostructure obtained after being immersed in a reduction agent hydrazine hydrate (HyH) with various concentrations of (a) 0.01 M, (b) 0.1 M, and (c) 1.0 M at a constant concentration (0.01 M) of silver nitrate ($AgNO_3$). The strong peak was acquired after investigating the diffraction peak along with the (111) plane at the value of 2θ (38.00), and the remaining peaks appeared with low intensity such as the (200) plane at the value of 2θ (44.28), (220) plane at the value of 2θ (64.60), as well as (311) plane at the value of 2θ (77.50). All the captured peaks of Ag were known as compared to the Joint Committee on Powder Diffraction Standards (JCPDS) silver card No, (04 - 0783). This demonstrates that the silver thin film nanostructure created by the SILAR technique was crystalline and had a face-centered cubic structure. It is established that the film is made entirely of silver because no further peaks of silver oxide or silver hydroxide could be seen in the diffraction pattern [24]. The crystallite size (D) of our material silver thin film nanostructure can be calculated for the detected peak diffraction such as (111), (200), (220), and (311) planes by using the Debye - Scherrer formula [25], as listed in Table 2.

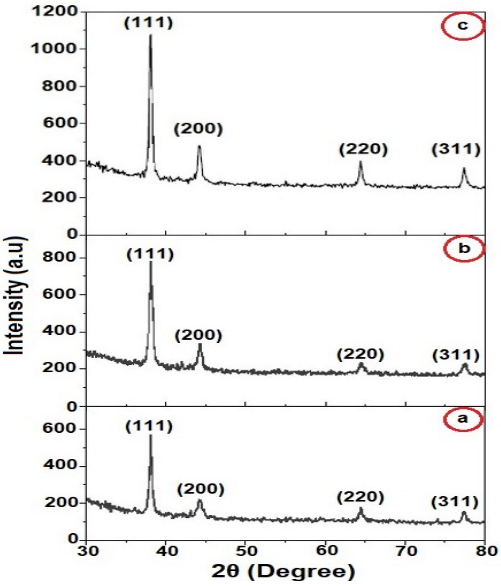

Figure 2. Shows X-Ray Diffraction (XRD) pattern of Ag thin film nanostructure captured after being submerged in a reduction agent hydrazine hydrate (HyH) with various concentrations of (a) 0.01 M, (b) 0.1 M, and (c) 1.0 M at a constant concentration (0.01 M) of silver nitrate ($AgNO_3$).

Table 2. XRD analysis of Silver thin film nanostructure.

Peak Diffractions	**(111)**	**(200)**	**(220)**	**(311)**
2θ	38.00	44.28	64.60	77.50
FWHM	0.3826	0.5542	0.4364	0.6356
Crystallite size (D) in nm	21.9	15.4	28.7	25.1
The average crystallite size (D_{ave}) in nm	22.775			

$$D = \frac{K\lambda}{\beta \cos\theta} \qquad (6)$$

Where, (K) is the Debye - Scherrer constant (0.9) for spherical crystallites with cubic symmetry, (D) is the crystallite size in nm, and (θ) is the Braggs angle in degrees, half of 2θ. (λ) is the X-Ray source wavelength. Cu Kα = 1.5406 A°, and (β) is the line broadening at full-width half maximum (FWHM) in radians.

3.2. Scanning Electron Microscope (SEM) analysis

Scanning electron microscopy (SEM) was utilized to examine the surface morphology of the grown Ag thin film nanoparticles using a JEOL JSM-6360A apparatus with high magnifications (x30000) and 20 kV operating voltage. Figure 3 demonstrates standard SEM images of silver thin film nanoparticles that were applied to the glass substrate at a constant concentration (0.01 M) of AgNO3 and with the various aqueous reduction concentrations of hydrazine hydrate (0.01 M, 0.1 M, 1.0 M) solution [26]. It has been noted that the particles are distributed evenly throughout the glass substrate, as can be seen in Figure 3(a). According to SEM, Figures 3 (b, c, and d) increasing the reduction concentration results in more Ag nanoparticles covering the whole glass substrate. The distribution of silver nanoparticles on the glass substrate and the size does not significantly vary for the reduction concentrations (0.1 M) and (1.0 M). It is clear from SEM figures that the majority of the produced Ag nanoparticles are spherical with a few larger non-spherical/rock-shaped particles, resulting in strong quadruple plasmon resonance. Ag nuclei are produced as a result of the adsorbed Ag+ ions being reduced. Since the amount of adsorbed Ag+ ions was constant, a greater reduction concentration led to the formation of more nuclei and, thus, a larger coverage. At 3 growing cycles, the majority of the Ag nanoparticles are spherical. Moreover, SEM images show that an increase in the reduction rate leads to an increase in the coverage of Ag nanoparticles over the entire glass substrate. It is evident from SEM images that most of the grown Ag nanoparticles are spherical with few exceptions of bigger and nonspherical Ag nanoparticles contributing to quadruple peaks. The reduction of the adsorbed Ag+ ions results in Ag particles. Because the number of the adsorbed Ag+ ions was fixed, with an increase in reduction agent concentration more particles were formed resulting in a higher coverage. When using the thermal evaporation method, it is well established that an increase in evaporation flux causes the distribution and the size of the produced nanoparticles to change [27].

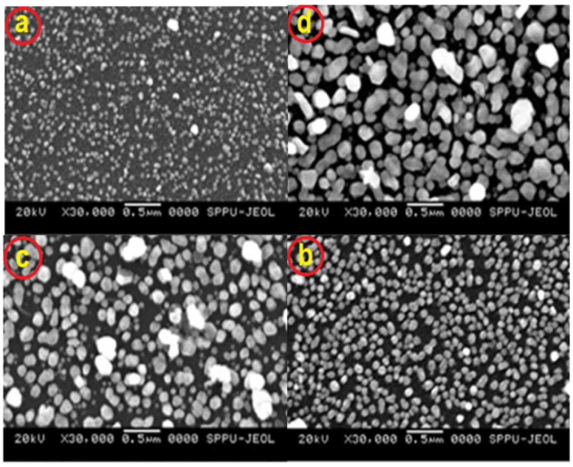

Figure 3. Illustrates Scanning Electron Microscope (SEM) images of Ag thin film nanoparticles at (a) constant concentration (0.01 M) of $AgNO_3$, and various reduction concentrations of (b) (0.01 M) conc. Of hydrazine hydrate, (c) (0.1 M) conc. Of hydrazine hydrate, and (d) (1.0 M) conc. Of hydrazine hydrate.

3.3. UV analysis of the thin film

The JASCO V-670 UV-Vis-NIR spectrophotometer was used to detect optical absorption of Ag thin film produced in the aqueous solution of hydrazine hydrate at various reduction concentrations (0.01, 0.1, 1.0) M as shown in Figure 4. These spectra show the appearance of a surface plasmon peak. The dipole Plasmon spectrum of nanocrystalline silver is located in the range of 386 to 422 nm. According to UV-Vis absorption spectra, the Surface Plasmon Resonance (SPR) peak gets stronger as the hydrazine hydrate concentration increases. Surface Plasmon Resonance occurs between 386 and 422 nanometers. The impact of the reduction rate on nucleation can be used to explain this event. The quantity and size of the particles produced by the reduction depending on the number of ions created at the start of the reaction [28]. Since there were initially few nuclei on the substrate at low concentrations of hydrazine hydrate due to the slow rate of reduction, this process continued and eventually led to the bigger size of particles. However, when the concentration of the hydrazine hydrate solution increases, the excess nuclei that were produced are reduced at a faster pace, which causes the formation of smaller, more agglomerated silver nanoparticles.

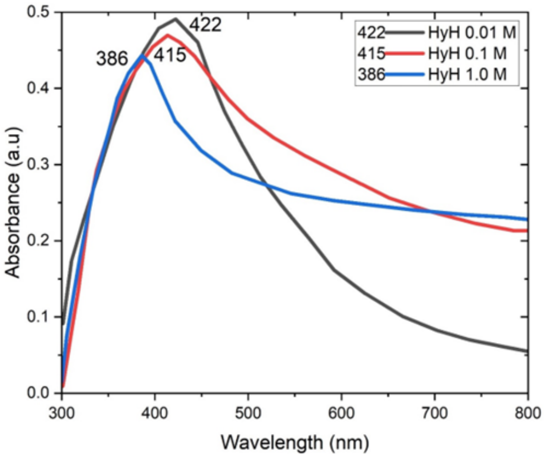

Figure 4. UV-Vis-NIR absorption spectra of silver thin film nanostructure were produced at several reduction agent concentrations (0.01, 0.1, and 1.0) M in an aqueous solution of hydrazine hydrate.

4. CONCLUSION

In this study, the SILAR method was successfully utilized to apply silver thin film nanoparticles on a large area of the glass substrate by using silver nitrate at constant concentration and various reduction agent concentrations in an aqueous solution of hydrazine hydrate. To achieve superior enhancement, the SILAR growth parameters (reduction agent, duration, and growth cycles) were optimized. The face-centered cubic structure of the nanostructured silver was proven by XRD. The size, surface area, and shape of the produced Ag nanoparticles alter as a result of changes in the SILAR growth parameters. At first, growth cycles enhance the size and surface area of spherical Ag nanoparticles; however, as growth cycles increase, the silver nanoparticles' shapes change to gravel or non-spherical. UV-Vis absorption spectra show that the strength of the Surface Plasmon Resonance (SPR) peak rises as the hydrazine hydrate concentration increases, mostly because of the variation in nucleation and growth activity. Moreover, silver nanoparticles are equally dispersed, as seen by SEM. It has been found that morphology, together with size and coverage, is a crucial aspect of the generated Ag nanoparticles in deciding the activity of growth cycles. Therefore, silver nanoparticles that have been produced with the ideal SILAR conditions can be employed as an extremely sensitive, repeatable substrate with an exceptionally efficient factor.

REFERENCES

[1] Khan, Saadbin, and M. Khalid Hossain. "Classification and properties of nanoparticles." In Nanoparticle-Based Polymer Composites, pp. 15-54. Woodhead Publishing, 2022.

[2] Jamkhande, Prasad Govindrao, Namrata W. Ghule, Abdul Haque Bamer, and Mohan G. Kalaskar. "Metal nanoparticles synthesis: An overview on methods of preparation, advantages and disadvantages, and applications." Journal of drug delivery science and technology 53 (2019): 101174.

[3] Zhao, Chang-Xin, Jia-Ning Liu, Juan Wang, Ding Ren, Bo-Quan Li, and Qiang Zhang. "Recent advances of noble-metal-free bifunctional oxygen reduction and evolution electrocatalysts." Chemical Society Reviews 50, no. 13 (2021): 7745-7778.

[4] Sajid, Muhammad, and Justyna Płotka-Wasylka. "Nanoparticles: Synthesis, characteristics, and applications in analytical and other sciences." Microchemical Journal 154 (2020): 104623.

[5] Roto, Roto, Hani Prima Rasydta, Adhitasari Suratman, and Nurul Hidayat Aprilita. "Effect of reducing agents on physical and chemical properties of silver nanoparticles." Indonesian Journal of Chemistry 18, no. 4 (2018): 614-620.

[6] Gul, Nouroze, Sadia Ata, Ismat Bibi, Muhammad Azam, Abubaker Shahid, Norah Alwadai, Nasir Masood, and Munawar Iqbal. "Size controlled synthesis of silver nanoparticles: a comparison of modified Turkevich and BRUST methods." Zeitschrift für Physikalische Chemie 236, no. 9 (2022): 1173-1189.

[7] Stetsyshyn, Yurij, Kamil Awsiuk, Viktor Kusnezh, Joanna Raczkowska, Benedykt R. Jany, Andrij Kostruba, Khrystyna Harhay et al. "Shape-Controlled synthesis of silver nanoparticles in temperature-responsive grafted polymer brushes for optical applications." Applied Surface Science 463 (2019): 1124-1133.

[8] Cheon, Ja Young, Su Jun Kim, Young Ha Rhee, Oh Hyeong Kwon, and Won Ho Park. "Shape-dependent antimicrobial activities of silver nanoparticles." International journal of nanomedicine 14 (2019): 2773.

[9] Khodashenas, Bahareh, and Hamid Reza Ghorbani. "Synthesis of silver nanoparticles with different shapes." Arabian Journal of Chemistry 12, no. 8 (2019): 1823-1838.

[10] Rauwel, Protima, Erwan Rauwel, Stanislav Ferdov, and Mangala P. Singh. "Silver nanoparticles: Synthesis, properties, and applications." Advances in Materials Science and Engineering 2015 (2015).

[11] Zhang, Zhenglong, Chengyun Zhang, Hairong Zheng, and Hongxing Xu. "Plasmon-driven catalysis on molecules and nanomaterials." Accounts of chemical research 52, no. 9 (2019): 2506-2515.

[12]Henry, Johnson, Arockiasamy Ajaypraveenkumar, Ganesan Sivakumar, and Kannusamy Mohanraj. "A new approach for deposition of silver film from AgCl through successive ionic layer adsorption and reaction technique." Journal of Central South University 24, no. 12 (2017): 2793-2798.

[13] Shaikh, Imran M., and Shrikrishna D. Sartale. "SILAR grown Ag nanoparticles as an efficient large area SERS substrate." Journal of Raman Spectroscopy 49, no. 8 (2018): 1274-1287.

[14] Desai, Mangesh A., and S. D. Sartale. "Facile soft solution route to engineer hierarchical morphologies of ZnO nanostructures." Crystal Growth & Design 15, no. 10 (2015): 4813-4820.

[15] Lee, Jae-Chul, Wansun Kim, Hun-Kuk Park, and Samjin Choi. "Controlling successive ionic layer absorption and reaction cycles to optimize silver nanoparticle-induced localized surface plasmon resonance effects on the paper strip." Spectrochimica Acta Part A: Molecular and Biomolecular Spectroscopy 174 (2017): 37-43.

[16] Yi, Zonghui, and Jiangping Cao. "Controllable Preparation and Characterization of Silver Nanoparticles." In 2018 3rd International Workshop on Materials Engineering and Computer Sciences (IWMECS 2018), pp. 71-74. Atlantis Press, 2018.

[17] Kim, Wansun, Yeon-Hee Kim, Hun-Kuk Park, and Samjin Choi. "Facile fabrication of a silver nanoparticle immersed, surface-enhanced Raman scattering imposed paper platform through successive ionic layer absorption and reaction for on-site bioassays." ACS applied materials & interfaces 7, no. 50 (2015): 27910-27917.

[18] Mukherji, Suparna, Sharda Bharti, Gauri Shukla, and Soumyo Mukherji. "Synthesis and characterization of size-and shape-controlled silver nanoparticles." Physical Sciences Reviews 4, no. 1 (2019).

[19] Lin, Jian-Yang, Yu-Lee Hsueh, Jung-Jie Huang, and Jia-Rung Wu. "Effect of silver nitrate concentration of silver nanowires synthesized using a polyol method and their application as transparent conductive films." Thin Solid Films 584 (2015): 243-247.

[20] Dhahir, D. M., A. J. K. Alrubaie, K. A. Mohammed, A. S. Baron, M. M. Abood, and A. H. O. Alkhayatt. "The role of Ag layer in the optical properties of PN junction thin films." Chalcogenide Letters 19, no. 3 (2022).

[21] Mitkari, A. V., and A. U. Ubale. "Thickness dependent physical properties of SILAR deposited nanostructured CoS thin films." ES Materials & Manufacturing 5 (2019): 49-56.

[22] Bartenbach, Daniel, Olivia Wenzel, Radian Popescu, Lara-Pauline Faden, Andreas Reiß, Michelle Kaiser, Anna Zimina, Jan-Dierk Grunwaldt, Dagmar Gerthsen, and Claus Feldmann. "Liquid-Phase Synthesis of Highly Reactive Rare-Earth Metal Nanoparticles." Angewandte Chemie International Edition 60, no. 32 (2021): 17373-17377.

[23] Ansari, A. A., and S. D. Sartale. "Controlled growth of thermally stable uniform-sized Ag nanoparticles on flat support and their electrochemical activity." Applied Physics A 119, no. 2 (2015): 503-516.

[24] Diantoro, Markus, Alif Fitria Chasanah, Nandang Mufti, and Abdulloh Fuad. "Fabrication of Silver Nanoparticles and Its Films and Their Characterization of Structure and Electrical Conductivity." In Advanced Materials Research, vol. 896, pp. 341-346. Trans Tech Publications Ltd, 2014.

[25] Epp, J. "X-ray diffraction (XRD) techniques for materials characterization." In Materials characterization using nondestructive evaluation (NDE) methods, pp. 81-124. Woodhead publishing, 2016.

[26] Abbas, Naseem, Muhammad Rizwan Shad, Muzamil Hussain, Syed Muhammad Zain Mehdi, and Uzair Sajjad. "Fabrication and characterization of silver thin films using physical vapor deposition, and the investigation of annealing effects on their structures." Materials Research Express 6, no. 11 (2019): 116437.

[27] Zhang, Jie, Xiaolei Zhang, Simeng Chen, Tiancheng Gong, and Yong Zhu. "Surface-enhanced Raman scattering properties of multi-walled carbon nanotubes arrays-Ag nanoparticles." Carbon 100 (2016): 395-407.

[28] Alsubaie, Haya, Zoya Zaheer, and Elham Shafik Aazam. "Role of ionic surfactants on the nucleation and growth of silver nanoparticles." Journal of Molecular Liquids 341 (2021): 117309.